Tides in the Ulleung Basin of the Japan/East Sea

J. W. Book (Naval Research Laboratory),
M. Wimbush, J.-H. Park, K.L. Tracey, and D. R. Watts (University of Rhode Island)

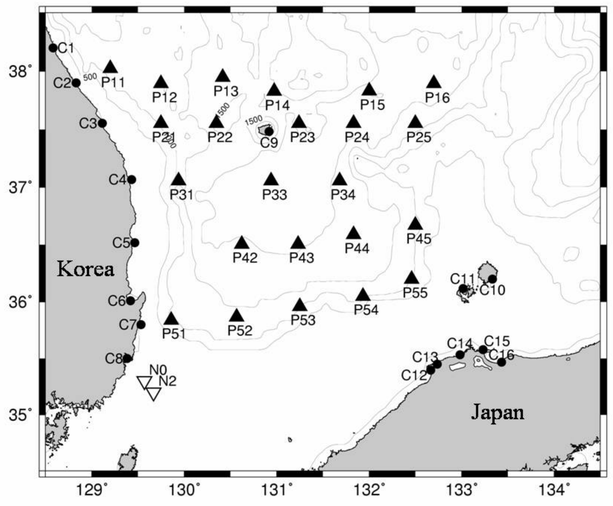

Ulleung Basin Tide Data

From June 1999 to June 2001, 23 pressure-sensor-equipped inverted echo sounders (PIES) were deployed in a 2-D array covering the Ulleung Basin (UB) of the Japan/East Sea ("P" sites in the above figure). The main purpose of the study was the temporal mapping of the thermal structure of the UB. However, tidal pressure fluctuations were also measured by this array. The poster presents this aspect of the study. Tidal pressure fluctuations were extracted from the pressure time series by using the the Munk and Cartwright (1966) response method.

Other tidal data for this region are available and are being used in this study. Data from 16 coastal tide stations were obtained from the International Hydrographic Office ("C" sites in the above figure). The duration of the measurements varied from site to site but every site had amplitude and phase values for at least the O_1, K_1, M_2, and S_2 tides. In addition to the coastal tide data, we used 6-month data records from two "LINKS" bottom-mounted instruments (Teague et al., 2002) deployed in the northwestern part of the Korea/Tsushima Strait ("N" sites in the above figure). Both of these instruments contained an acoustic Doppler current profiler (ADCP) and one of them contained a pressure gage. We applied harmonic analysis to determine, from the LINKS measurements, tidal constituent amplitudes and phases of both the vertically averaged current and the pressure.

Data Assimilation Model

A linear barotropic data assimilation model was run on a 5-km C-grid to generate dynamically consistent tidal predictions for the UB using the tidal data from the observational array. The forward (time-domain) model equations are the linear shallow water equations:

$$\frac{\partial u}{\partial t} = -g\frac{\partial \eta}{\partial x} + fv - \frac{\lambda}{h}u \qquad (1)$$

$$\frac{\partial v}{\partial t} = -g\frac{\partial \eta}{\partial y} - fu - \frac{\lambda}{h}v \qquad (2)$$

$$\frac{\partial \eta}{\partial t} + \frac{\partial hu}{\partial x} + \frac{\partial hv}{\partial y} = 0 \qquad (3)$$

u and v are the eastward (x) and northward (y) velocities respectively, η is the surface height, t is time, g is the gravitational acceleration, f is the Coriolis parameter, h is the depth, and λ is a frictional parameter (3×10^{-3} m/s).

Optimized Boundary Forcing

The open ocean boundary conditions are,

$$U_B = \frac{F}{h} \mp \alpha\,\eta_B\,, \qquad (4)$$

where U_B is the normal velocity at a boundary, α is an admittance coefficient, and η_B is the internal model surface height closest to the boundary. The first term is a forcing term and the second term is a radiation term. The forcing F is commonly provided by tide charts or larger models for many regional tide modeling studies. However the tide charts and the larger models may have significant errors which will then be propagated into the regional model. We instead infer the time series F from our observations using an inverse technique. A cost function (J) provides a weighted (w) measure of how well a particular model run's predictions (p) match the observed data set (m):

$$J = \sum_{i,j} w_i\left(m_{i,j} - p_{i,j}\right)^2, \qquad (5)$$

where i is a station index and j a time index. The cost function, equation 5, is implicitly a function of the F terms from equation 4. We assume F is uniform along each of 17 boundary sections (shown as alternating black and gray bands in the figure at the bottom of this column). Choosing these 17 values at each time step completely determines the values of p and thus J. We therefore minimize J with respect to F with equations 1-3 as strong constraints. This technique attempts to match observed values of u, v, and η by adjusting the forcing along the model boundary. The resulting solution is constrained to follow the discrete form of the dynamical equations everywhere within the model domain.

Prediction Errors

The figure below shows the estimated model prediction error for the M_2 surface-height amplitude calculated from standard regression analysis. The error is less than 0.002 m for most of the domain which is about 1/20th of typical M_2 amplitudes in the UB.

The figure at the top of the next column shows rms differences between observed tidal time series and model predictions. These differences are typically 0.007 m and 0.013 m for surface heights at the PIES sites and coastal tide stations, respectively, and 0.03 m/s at the two ADCP sites.

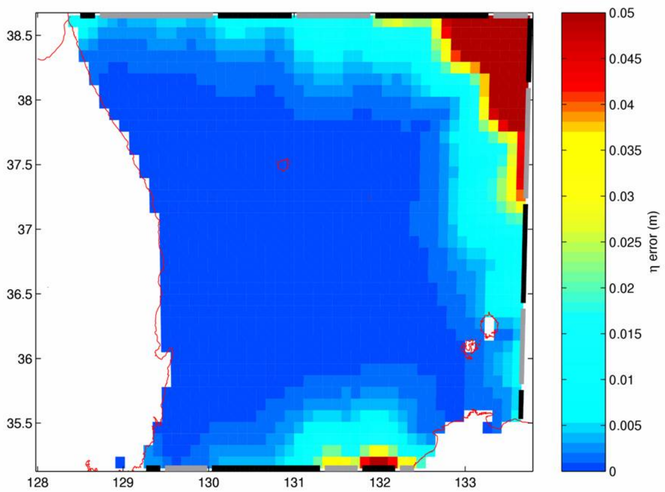

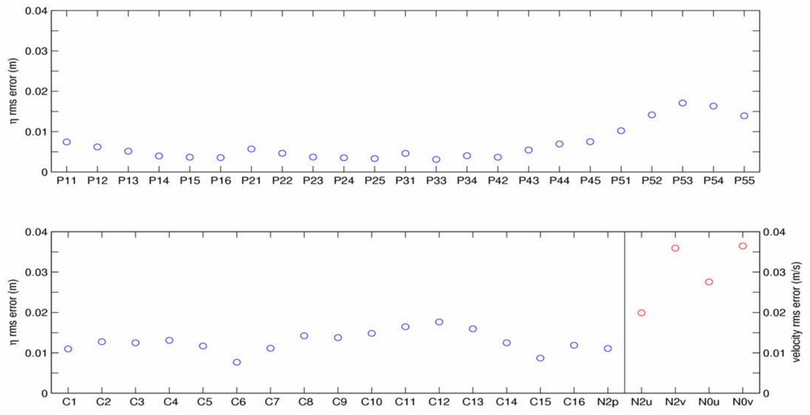

Model Solutions

The time-domain output from the model is harmonically analyzed at each grid point to determine the amplitude and phase of the tide constituents being considered. We show below the surface-height solutions for the O_1, K_1, M_2 and S_2 constituents. It is apparent that each of these constituents has an amphidromic point either within the modeled region or just outside, in the Korea-Tsushima Strait to the south. These results are in agreement with those from a similar data-assimilation model for the Korea-Tsushima Strait region (Book et al., 2003).

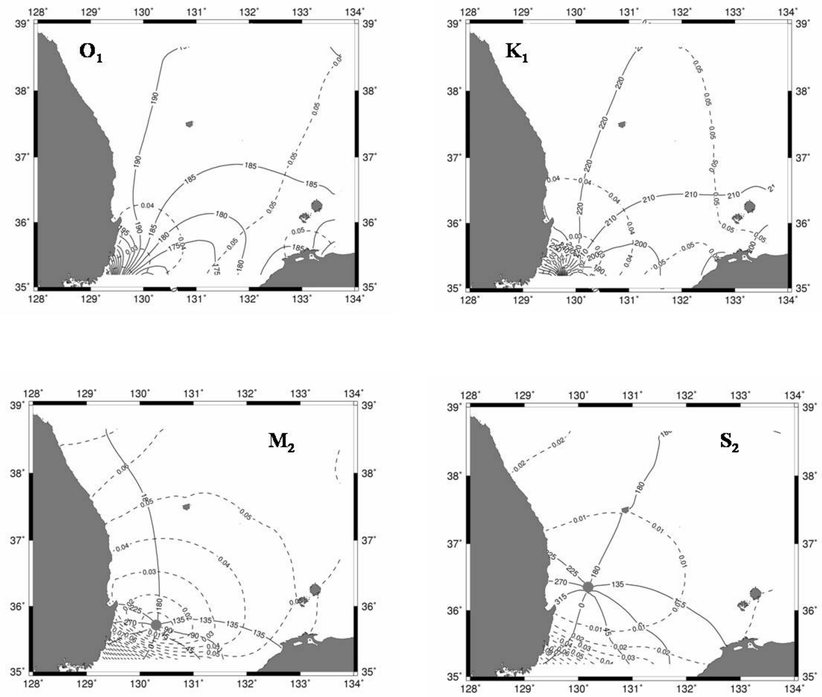

References

Book, J.W., P. Pistek,, H.T. Perkins, K.R. Thompson, W.J. Teague, G.A. Jacobs, M-S. Suk, K-I Chang, J-C. Lee and B-H., Choi, 2003. Data assimilation modeling of the barotropic tides in the Korea/Tsushima Strait. *J. Oceanog*, in revision.

Munk, W.H., and D. Cartwright, 1966. Tidal spectroscopy and prediction. *Phil. Trans. Roy. Soc. London, Series A*, **259**, 533-581.

Teague, W.J., G.A. Jacobs, H. T. Perkins, J. W. Book, K-I Chang and M-S. Suk, 2002. Low-frequency current observations in the Korea/Tsushima Strait. *J. Phys. Oceanog.*, **32**, 1621-1641.